Supporting Information

Structural, Electrochemical and Catalytic Elucidation of Cyclooctadiene Ru(II)-Nitrile Complexes of the Type $[RuCl_2(cod)(NCR)_2]$

Frederick P. Malan*

Supporting Information

1. Experimental Section

General considerations. All experiments were performed under an argon atmosphere using standard Schlenk techniques. Solvents were dried and distilled from appropriate drying agents prior to use. The polymeric $[RuCl_2(cod)]_n$, as well as complexes **1** and **8** were synthesized according to previously reported methods.[1, 2] Other chemicals used were purchased from commercial suppliers and utilized without further purification. NMR spectroscopy: ^{1}H (400 MHz) and $^{13}C\{^{1}H\}$ (77 MHz) NMR spectra were recorded on either a Bruker Avance-400 or Bruker Avance-300 spectrometer using $CDCl_3$ unless otherwise stated. All measurements were performed at ambient temperature (298 K). Chemical shifts were referenced to the internal residual solvent resonances (δ_H = 7.24 ppm; δ_C = 77.0 ppm). Electrospray mass spectra (ESI-MS) were recorded on a micromassQuatro LC instrument. EA analyses were performed using a ThermoScientific Flash2000 Elemental Analyser.

General synthesis of complexes 2-11

A solution of **1** (362 mg, 1 mmol) in MeOH (10 mL) containing the respective nitrile (2.2 mmol) was stirred at 50°C for 1 hour. The resulting solution was concentrated *in vacuo*, to *ca.* 5 mL and left in the fridge (5 °C) to crystallize overnight. A range of yellow to orange crystals were obtained after subsequent filtration *in vacuo* and washing with Et_2O (2 × 5 mL).

2: Yield: 339 mg (87%). ^{1}H NMR ($CDCl_3$): δ_H = 1.42 (t, $^{3}J_{HH}$ = 12 Hz, 6H, CH_3), 1.99 (m, 4H, CH_2(cod)), 2.40 (m, 4H, CH_2(cod)), 2.90 (q, $^{3}J_{HH}$ = 12 Hz, 4H, CH_2), 4.21 (br s, 4H, CH(cod)). $^{13}C\{^{1}H\}$ NMR: δ_C = 10.2 (s, CH_3), 13.7 (s, CH_2), 29.6 (s, CH_2(cod)), 89.8 (s, CH(cod)), 129.6 (s, CN). HR-MS (ESI, m/z): calcd for $C_{14}H_{22}ClN_2Ru$ $[M - Cl]^+$, 355.0515; found 355.0518. CHN (%) found (calcd) for $C_{14}H_{22}Cl_2N_2Ru$: C, 43.02 (43.08), H, 5.74 (5.68), N, 6.96 (7.18)%.

3: Yield: 393 mg (95%). ^{1}H NMR ($CDCl_3$): δ_H = 2.00 (q, $^{3}J_{HH}$ = 4 Hz, 6H, CH_2(cod)), 2.41 (m, 4H, CH_2(cod)), 3.69 (dt, $^{3}J_{HH}$ = 5 Hz, 1 Hz, 4H, CH_2), 4.26 (br s, 4H, CH(cod)), 5.41 (d, $^{3}J_{HH}$ = 16 Hz, 2H, =CH), 5.70 (d, $^{3}J_{HH}$ = 16 Hz, 2H, $=CH_2$), 5.80 (m, 2H, $=CH_2$). $^{13}C\{^{1}H\}$ NMR: δ_C = 23.9 (s, CH_2), 29.4 (s, CH_2(cod)), 90.2 (s, CH(cod)), 119.8 (s, =CH), 121.6 (s, $=CH_2$), 126.6 (s, CN). HR-MS (ESI, m/z): calcd for $C_{16}H_{22}ClN_2Ru$ $[M - Cl]^+$, 379.0515; found 379.0529. CHN (%) found (calcd) for $C_{16}H_{22}Cl_2N_2Ru$: C, 45.69 (46.38), H, 5.61 (5.35), N, 6.93 (6.76)%.

4: Yield: 363 mg (87%). ^{1}H NMR ($CDCl_3$): δ_H = 1.46 (d, $^{3}J_{HH}$ = 8 Hz, 12H, CH_3), 1.98 (q, $^{3}J_{HH}$ = 8 Hz, 4H, CH_2(cod)), 2.39 (m, 4H, CH_2(cod)), 3.20 (sept, $^{3}J_{HH}$ = 8 Hz, 2H, C*H*Me_2), 4.17 (br s, 4H, CH(cod)). $^{13}C\{^{1}H\}$ NMR: δ_C = 19.7 (s, CH_3), 22.4 (s, $CHMe_2$), 29.4 (s, CH_2(cod)), 89.8 (s, CH(cod)), 132.6 (s, CN). HR-MS (ESI, m/z): calcd for $C_{16}H_{26}ClN_2Ru$ $[M - Cl]^+$, 383.0828; found 383.0862. CHN (%) found (calcd) for $C_{16}H_{26}Cl_2N_2Ru$: C, 46.17 (45.93), H, 5.87 (6.26), N, 6.87 (6.70)%.

5: Yield: 393 mg (94%). Yield: 363 mg (87%). ^{1}H NMR ($CDCl_3$): δ_H = 1.13 (t, $^{3}J_{HH}$ = 8 Hz, 6H, CH_3), 1.87 (sext, $^{3}J_{HH}$ = 8 Hz, 4H, CH_2), 1.98 (q, $^{3}J_{HH}$ = 12 Hz, 4H, CH_2(cod)), 2.39 (m, 4H, CH_2(cod)), 2.85 (t, $^{3}J_{HH}$ = 8 Hz, 4H, CH_2), 4.20 (br s, 4H, CH(cod)). $^{13}C\{^{1}H\}$ NMR: δ_C = 13.5 (s, CH_3), 19.2 (s, CH_2), 21.5 (s, CH_2), 29.4 (s, CH_2(cod)), 89.7 (s, CH(cod)), 129.0 (s, CN). HR-MS (ESI, m/z): calcd for $C_{16}H_{26}ClN_2Ru$ $[M - Cl]^+$, 383.0828; found 383.0802. CHN (%) found (calcd) for $C_{16}H_{26}Cl_2N_2Ru$: C, 46.31 (45.93), H, 6.45 (6.26), N, 6.38 (6.70)%.

6: Yield: 372 mg (88%). ^{1}H NMR ($CDCl_3$): δ_H = 2.00 (q, $^{3}J_{HH}$ = 8 Hz, 4H, CH_2(cod)), 2.46 (m, 4H, CH_2(cod)), 3.57 (s, 6H, OCH_3), 4.28 (br s, 4H, CH(cod)), 4.73 (s, 4H, CH_2). $^{13}C\{^{1}H\}$ NMR: δ_C = 29.3 (s, CH_2(cod)), 59.0 (s, CH_2), 60.0 (s, OCH_3), 90.8 (s, CH(cod)), 126.5 (s, CN). HR-MS (ESI, m/z): calcd for $C_{14}H_{22}ClN_2O_2Ru$ $[M - Cl]^+$, 387.0413; found 387.0461. CHN (%) found (calcd) for $C_{14}H_{22}Cl_2N_2O_2Ru$: C, 39.72 (39.82), H, 5.05 (5.25), N, 6.58 (6.63)%.

7: Yield: 414 mg (96%). ^{1}H NMR ($CDCl_3$): δ_H = 2.03 (m, 4H, CH_2(cod)), 2.46 (m, 4H, CH_2(cod)), 4.06 (d, $^{3}J_{HH}$ = 32 Hz, 1H, CH_2), 4.32 (d, $^{3}J_{HH}$ = 32 Hz, 1H, CH_2), 4.33 (br s, 4H, CH(cod)), 4.74 (s, 2H, CH_2). $^{13}C\{^{1}H\}$ NMR: δ_C = 29.2 (s, CH_2(cod)), 30.9 (s, CH_2), 90.0 (s,

CH(cod)). HR-MS (ESI, m/z): calcd for $C_{12}H_{16}Cl_3N_2Ru$ [M – Cl]$^+$, 394.9423; found 394.9404. CHN (%) found (calcd) for $C_{12}H_{16}Cl_4N_2Ru$: C, 33.41 (33.43), H, 3.88 (3.74), N, 6.55 (6.50)%.

9: Yield: 535 mg (83%). ^{1}H NMR ($CDCl_3$): δ_H = 2.12 (q, $^3J_{HH}$ = 8 Hz, 4H, CH_2(cod)), 2.55 (m, 4H, CH_2(cod)), 4.46 (br s, 4H, CH(cod)), 7.72 (dd, $^3J_{HH}$ = 12 Hz, 8 Hz, 8H, C_6H_4). $^{13}C\{^1H\}$ NMR: δ_C = 29.6 (s, CH_2(cod)), 91.0 (s, CH(cod)), 128.0 (s, CN), 132.6 (s, C_6H_4), 132.8 (s, C_6H_4), 133.4 (s, C_6H_4), 134.1 (s, C_6H_4). HR-MS (ESI, m/z): calcd for $C_{22}H_{20}Br_2ClN_2Ru$ [M – Cl]$^+$, 608.8705; found 608.8757. CHN (%) found (calcd) for $C_{22}H_{20}Br_2Cl_2N_2Ru$: C, 40.63 (41.02), H, 3.18 (3.13), N, 4.70 (4.35)%.

9b: Obtained as a precipitate from the filtrate of **C9** after standing for 3 days. Yield: 59 mg (8%). ^{1}H NMR ($CDCl_3$): δ_H = 2.09 (m, 8H, CH_2(cod)), 2.54 (m, 8H, CH_2(cod)), 4.42 (br s, 8H, CH(cod)), 7.64 (m, 8 Hz, 4H, C_6H_4). $^{13}C\{^1H\}$ NMR: δ_C = 29.4 (s, CH_2(cod)), 91.0 (s, CH(cod)), 131.7 (s, C_6H_4), 132.8 (s, C_6H_4), 133.3 (s, C_6H_4), 134.4 (s, C_6H_4). HR-MS (ESI, m/z): calcd for $C_{23}H_{28}BrCl_3NRu_2$ [M – Cl]$^+$, 703.8556; found 703.8591. CHN (%) found (calcd) for $C_{23}H_{28}BrCl_4NRu_2$: C, 37.31 (37.21), H, 3.96 (3.80), N, 2.34 (1.89)%.

10: Yield: 442 mg (86%). ^{1}H NMR ($CDCl_3$): δ_H = 1.89 (q, $^3J_{HH}$ = 8 Hz, 4H, CH_2(cod)), 2.24 (m, 4H, CH_2(cod)), 4.26 (br s, 4H, CH(cod)), 4.30 (s, 4H, CH_2), 7.35 (m, 8H, C_6H_5), 7.46 (m, 2H, C_6H_5). $^{13}C\{^1H\}$ NMR: δ_C = 23.6 (s, CH_2), 29.3 (s, CH_2(cod)), 90.7 (s, CH(cod)), 127.9 (s, CN), 128.3 (s, C_6H_5), 128.8 (s, C_6H_5), 129.1 (s, C_6H_5), 129.8 (s, C_6H_5). HR-MS (ESI, m/z): calcd for $C_{24}H_{26}ClN_2Ru$ [M – Cl]$^+$, 479.0828; found 479.0877. CHN (%) found (calcd) for $C_{24}H_{26}Cl_2N_2Ru$: C, 56.09 (56.03), H, 5.04 (5.09), N, 5.64 (5.45)%.

11: Yield: 543 mg (93%). ^{1}H NMR ($CDCl_3$): δ_H = 1.93 (m, 4H, CH_2(cod)), 2.29 (m, 4H, CH_2(cod)), 4.26 (br s, 4H, CH(cod)), 4.31 (s, 4H, CH_2), 7.35 (d, $^3J_{HH}$ = 8 Hz, 4H, C_6H_4), 7.44 (d, $^3J_{HH}$ = 8 Hz, 4H, C_6H_4). $^{13}C\{^1H\}$ NMR: δ_C = 23.2 (s, CH_2), 29.3 (s, CH_2(cod)), 90.3 (s, CH(cod)), 127.1 (s, CN), 127.3 (s, C_6H_5), 129.2 (s, C_6H_5), 129.6 (s, C_6H_5), 134.6 (s, C_6H_5). HR-MS (ESI, m/z): calcd for $C_{24}H_{24}Cl_3N_2Ru$ [M – Cl]$^+$, 547.0049; found 547.0007. CHN (%) found (calcd) for $C_{24}H_{24}Cl_4N_2Ru$: C, 49.52 (49.41), H, 4.40 (4.15), N, 5.14 (4.80)%.

Catalysis

General procedure for catalytic runs evaluated: To an NMR tube containing the substrate (0.1 mmol), anisole as internal standard (11 µl, 0.1 mmol), ruthenium complex (3-5 mol%) was added, along with solvent/reagent (eg. ^{i}PrOH or BnOH (100 µL), H_2SiPh_2 (0.11 mmol)), as well as KO^{t}Bu (10 mol%) along with 0.8 mL C_6D_6. ^{1}H NMR spectroscopy was done at time = 0 followed by placing the tightly sealed vessel in an oil bath at 80°C for a determined

amount of time. A ^{1}H NMR spectrum was taken shortly after the removal of the NMR tube from the oil bath. Conversions were determined relative to anisole as the internal standard with the runs being performed in duplicate. TOF was determined by using the conversion determined after the first 10 minutes of the reaction.

X-ray Crystallography

Single crystals of all complexes were analyzed on a Rigaku XtaLAB Synergy R diffractometer, with a rotating-anode X-ray source and a HyPix CCD detector. Data reduction and absorption were carried out using the CrysAlisPro (version 1.171.40.23a) software package.[3] All X-ray diffraction measurements were performed at 150(1) K, using an Oxford Cryogenics Cryostat. Structures were solved by direct methods with SHELXTS-2013[4] and refined using the SHELXL-2013[5] algorithm. All H atoms were placed in geometrically idealized positions and constrained to ride on their parent atoms. For data collection and refinement parameters, see the SI (**Tables S1**-**S5**). The X-ray crystallographic coordinates for all structures have been deposited at the Cambridge Crystallographic Data Centre (CCDC), with deposition numbers CSD 2150078-2150089. The data can be obtained free of charge from The Cambridge Crystallographic Data Centre *via* www.ccdc.cam.ac.uk/data_request/cif.

Electrochemistry

Cyclic voltammetry (CV) and linear sweep voltammetry (LSV) measurements were conducted on a Metrohm μAutolab type III potentiostat, using NOVA 2.0 electrochemistry software. Measurements were made using 0.002 or saturated mol.dm^{-3} solutions of the complexes in dry dichloromethane containing 0.1 mol.dm^{-1} tetra-N-butylammonium hexafluorophosphate, [NBu_4][PF_6], as supporting electrolyte under a purified argon atmosphere at 25 °C. A three electrode cell, with a glassy carbon (surface area = 7.07 × 10^{-6} m^2) working electrode, a Pt auxiliary electrode, and a Ag wire as reference electrode, was used. Successive experiments under identical experimental conditions revealed all redox potentials were reproducible within 5 mV. All reported potentials were referenced against the saturated calomel electrode (SCE) using the FcH/FcH^+ couple as standard. Ferrocene exhibited a formal reduction potential of $E^{0'}$ = 0.381 V *vs.* Ag/Ag^+, a peak separation of ΔEp = Epa – Epc = 0.071 V, and i_{pa}/i_{pc} = 1.00, under the current experimental conditions. Epa (Epc) = anodic (cathodic) peak potential and ipa (ipc) = anodic (cathodic) peak current. The $E^{0'}$ of ferrocene (Fc/Fc^+) is reported to be 0.644 V *vs.* SCE.[6] Linear sweep voltammogram

(LSV) measurements were taken at a stationary electrode using a very slow scan rate of 2 mVs^{-1}.

Computational chemistry

All calculations were carried out in the gas phase using DFT with the B3LYP hybrid functional as implemented in the gas phase using the Gaussian 16 program[7]. The basis set def2-tzvpp[8] in conjunction with Grimme's D3 empirical dispersion correction[9] was used for all atoms, where in addition the Stuttgart/Dresden (SDD) pseudopotential was used to describe the ruthenium electronic core. All geometries were optimized without any symmetry restrictions, ensuring that the local minima had zero imaginary vibrational frequencies. Orbital and spin density plots were generated using Chemcraft[10] using isovalues of 0.06 (MOs) and 0.03 (spin).

2. Selected ^{1}H and ^{13}C NMR spectra of the ruthenium complexes (Figures S1-S20).

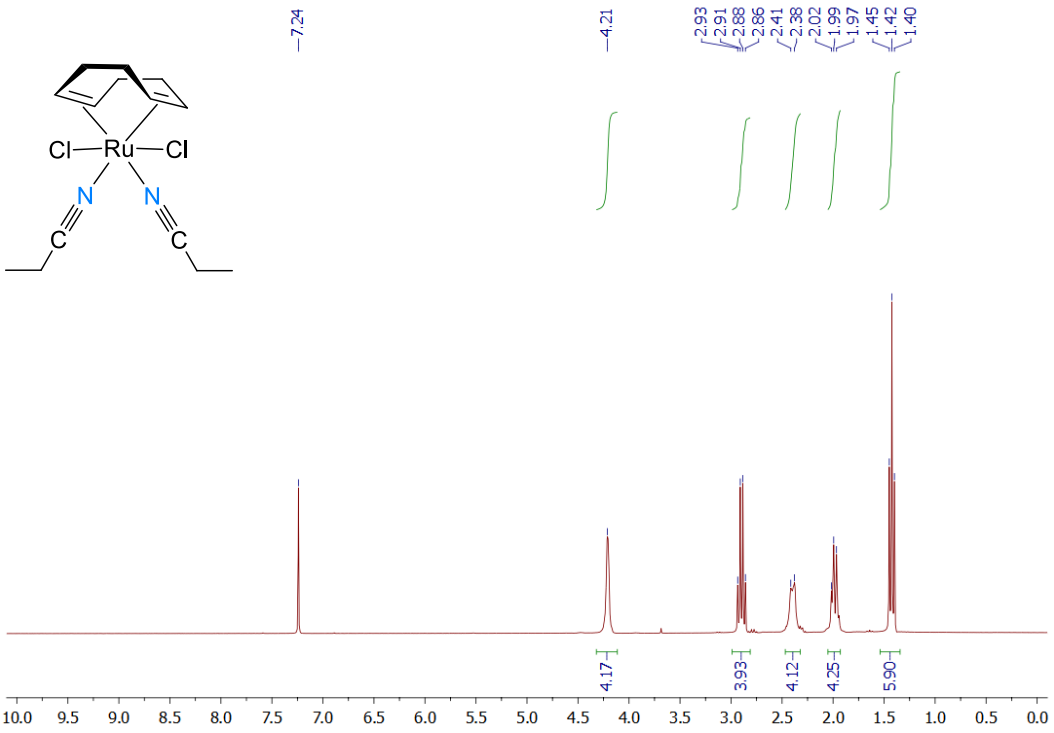

Figure S1 Complex **2**: ^{1}H NMR spectrum

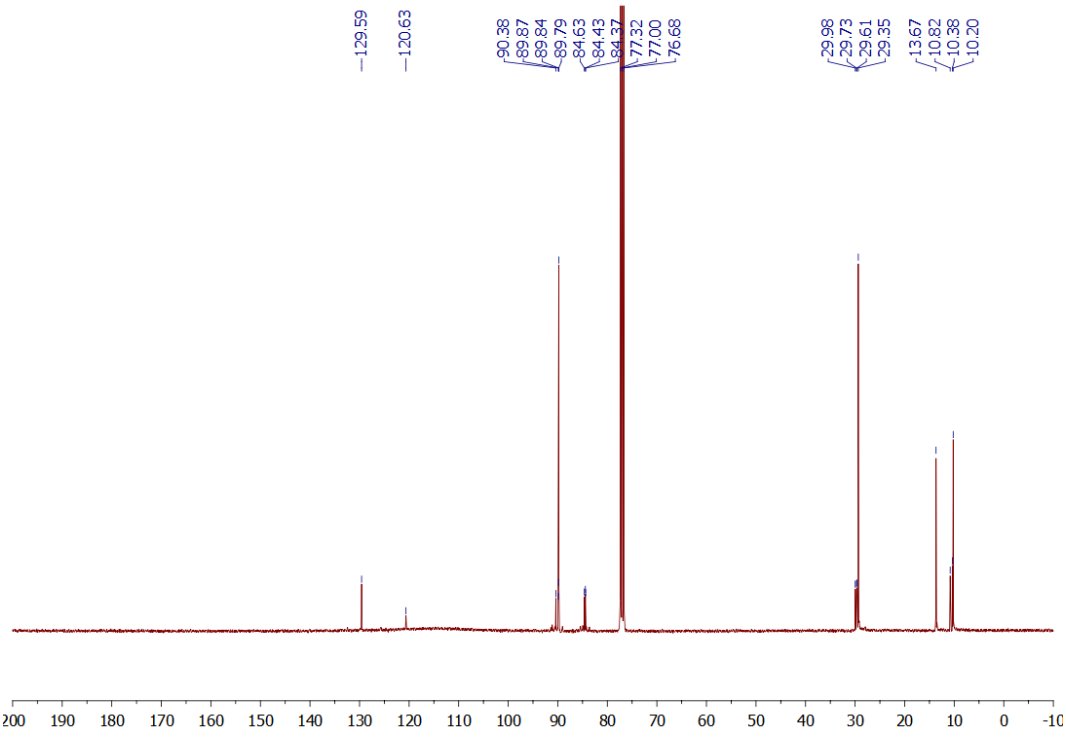

Figure S2 Complex **2**: ^{13}C NMR spectrum

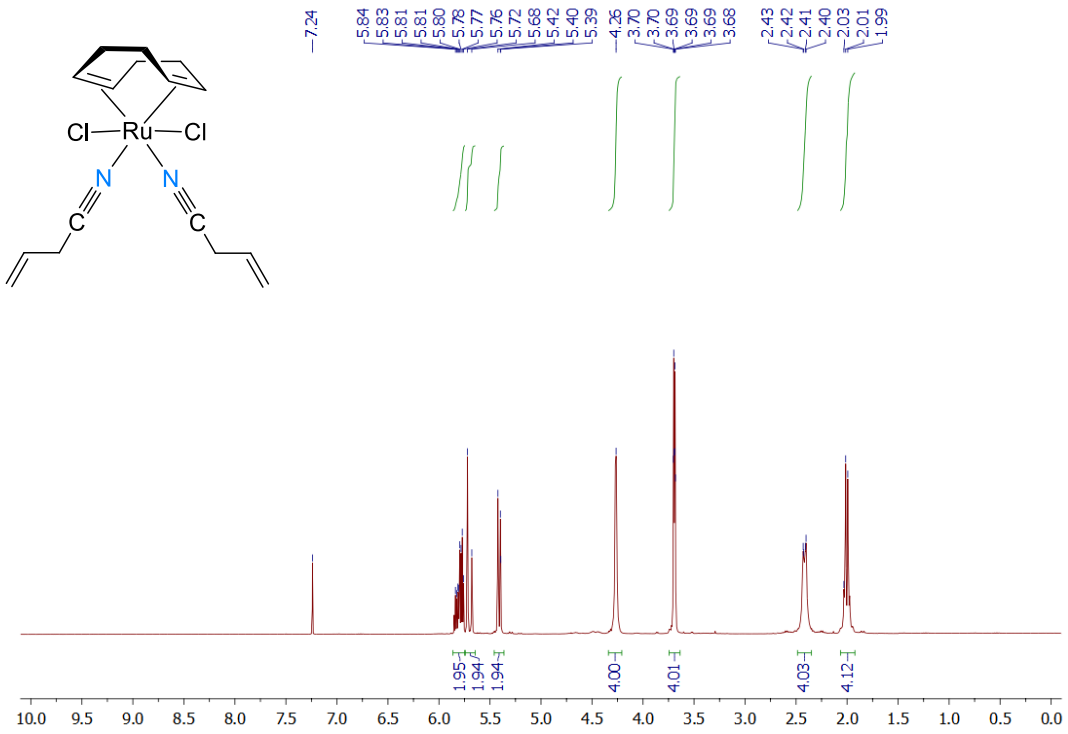

Figure S3 Complex **3**: ^{1}H NMR spectrum

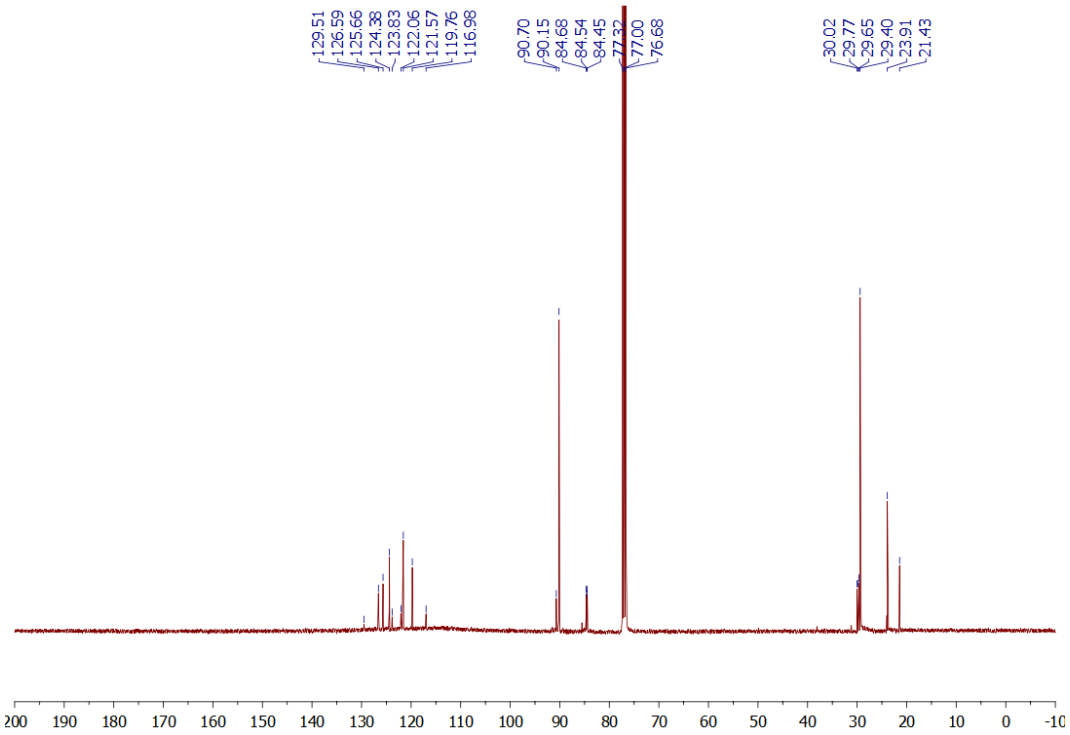

Figure S4 Complex **3**: ^{13}C NMR spectrum

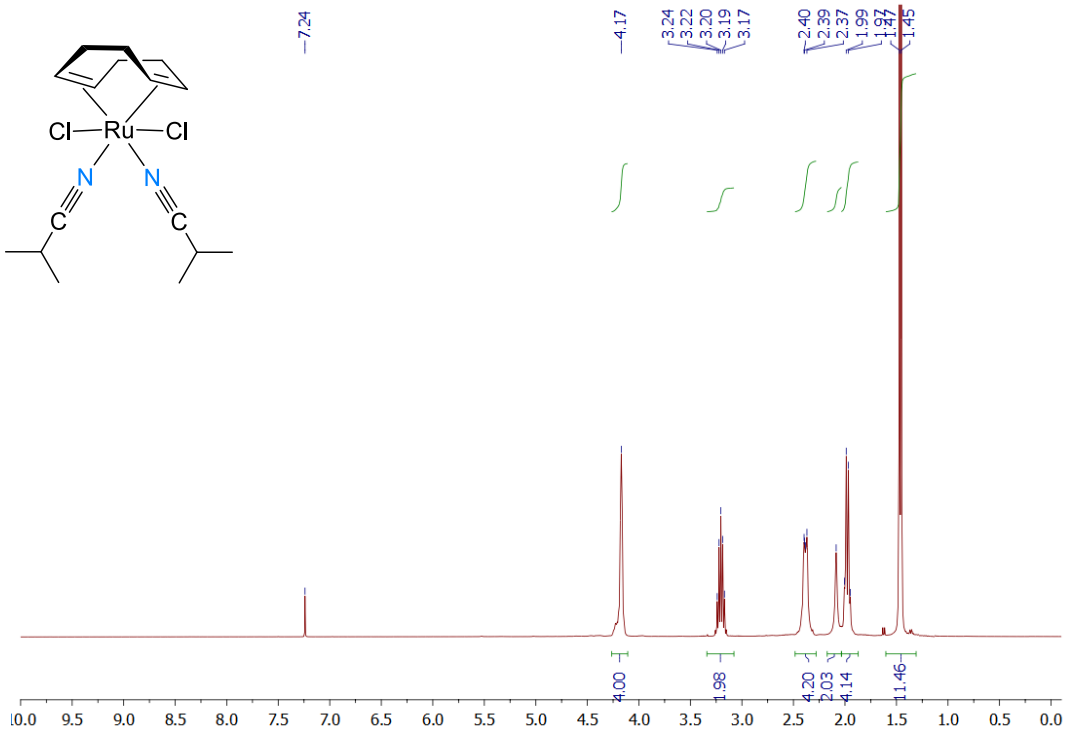

Figure S5 Complex **4**: ^{1}H NMR spectrum

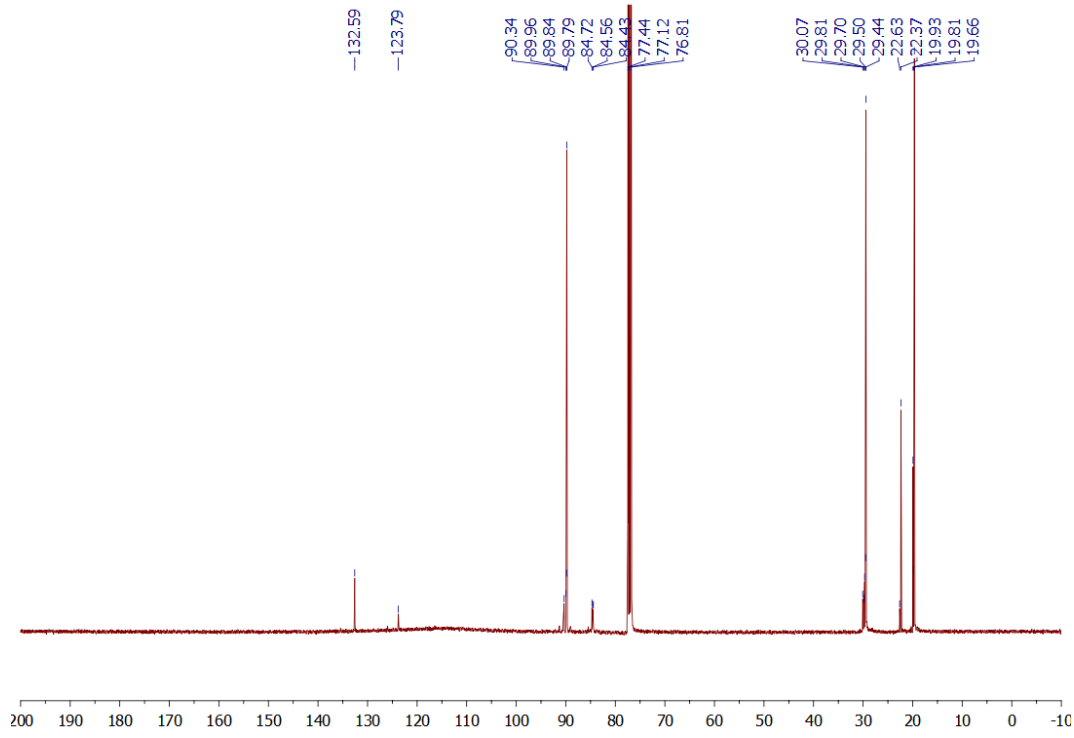

Figure S6 Complex **4**: ^{13}C NMR spectrum

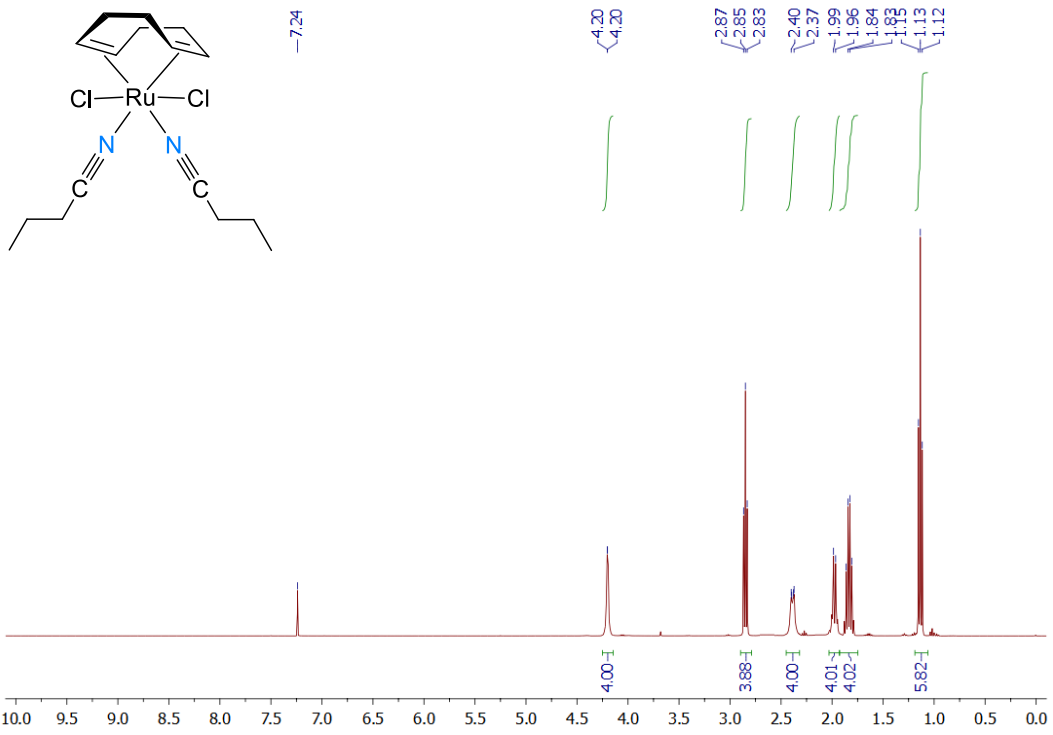

Figure S7 Complex **5**: ^{1}H NMR spectrum

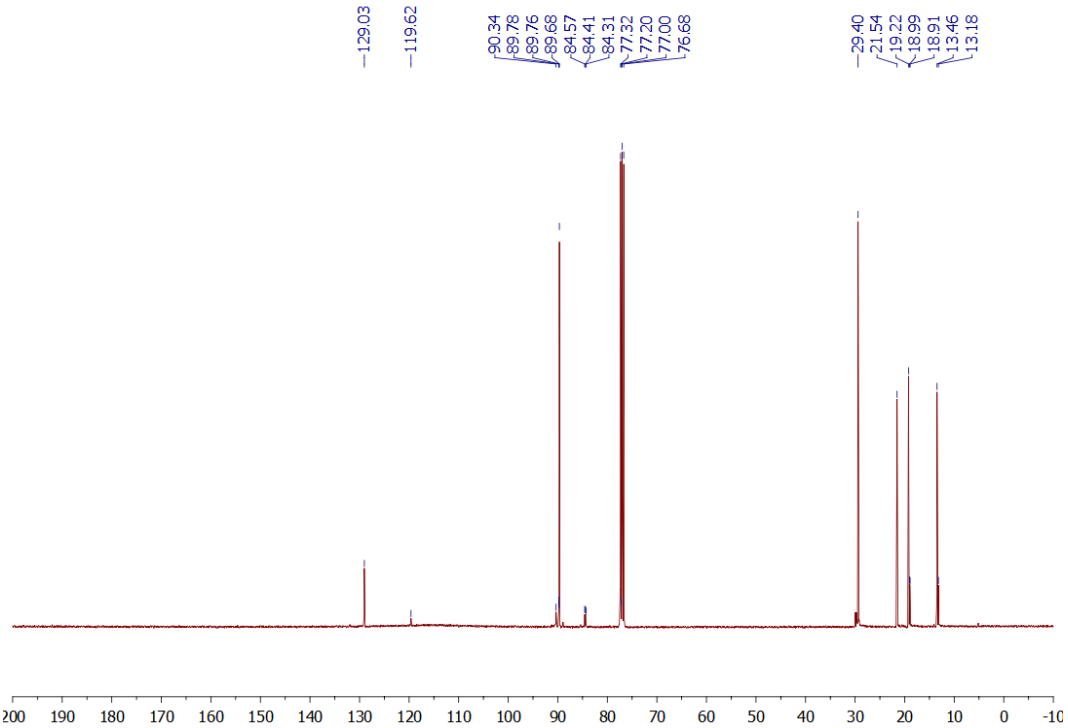

Figure S8 Complex **5**: ^{13}C NMR spectrum

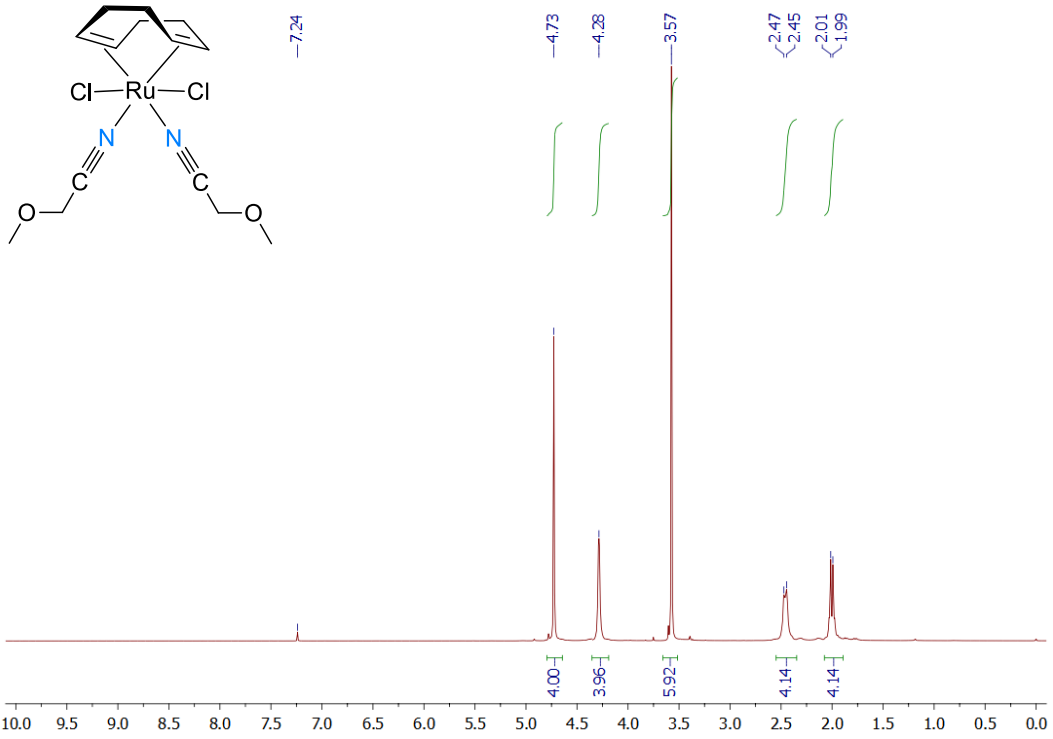

Figure S9 Complex **6**: ^{1}H NMR spectrum

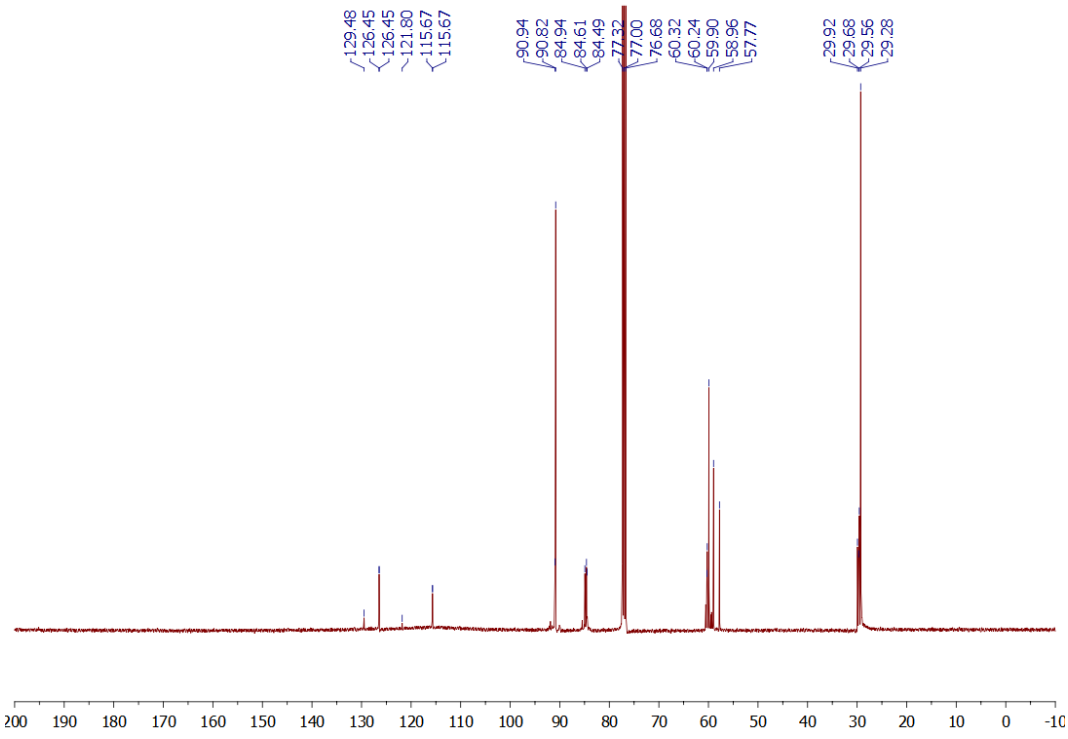

Figure S10 Complex **6**: ^{13}C NMR spectrum

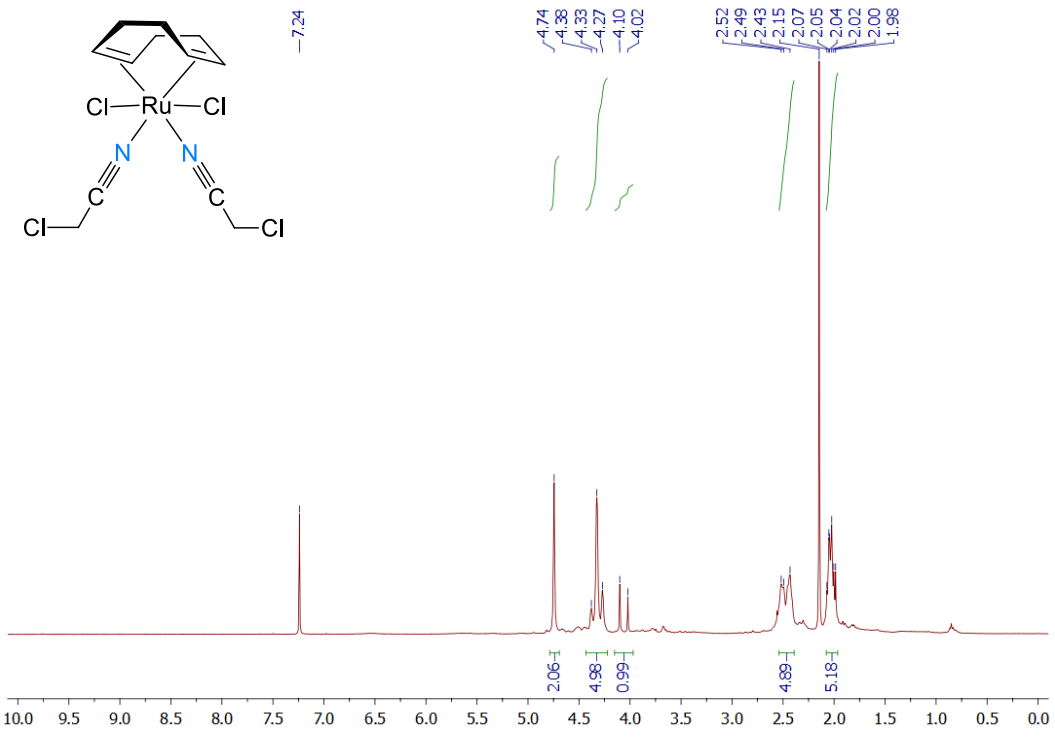

Figure S11 Complex **7**: ^{1}H NMR spectrum

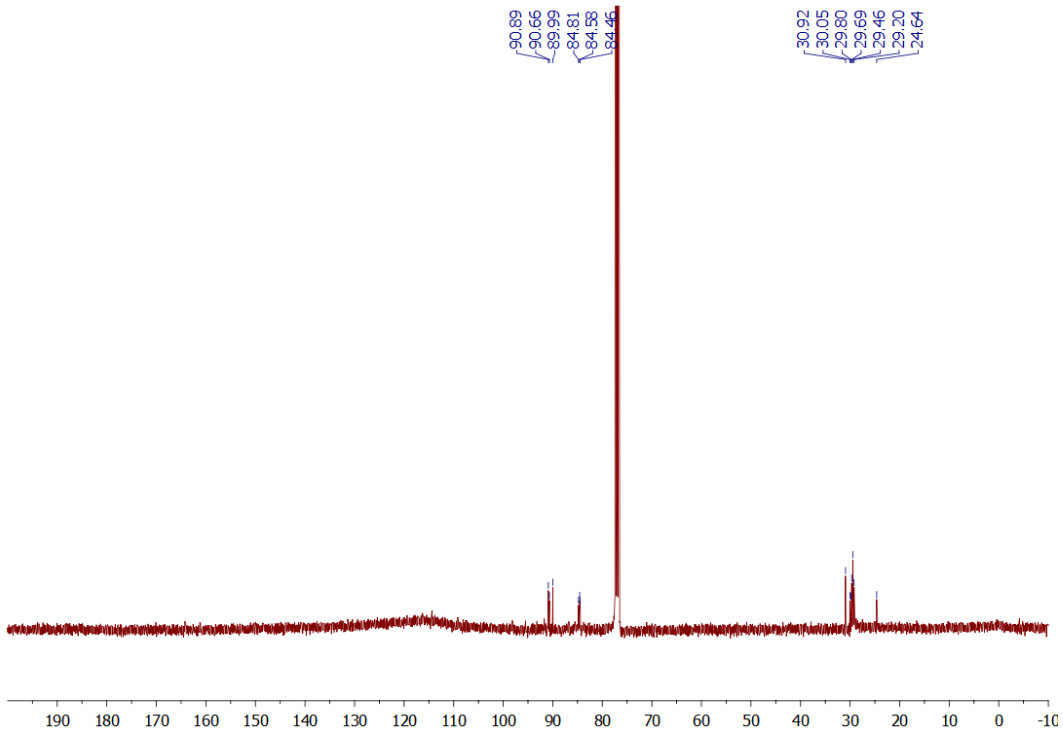

Figure S12 Complex **7**: ^{13}C NMR spectrum

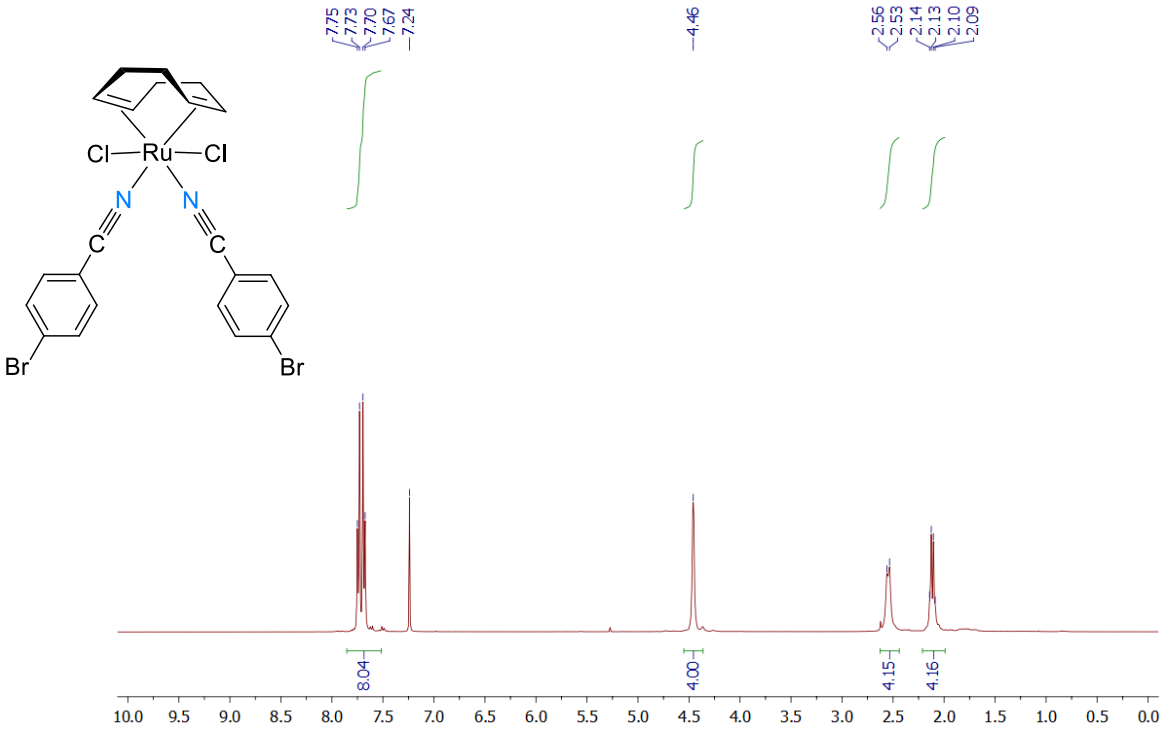

Figure S13 Complex **9**: ^{1}H NMR spectrum

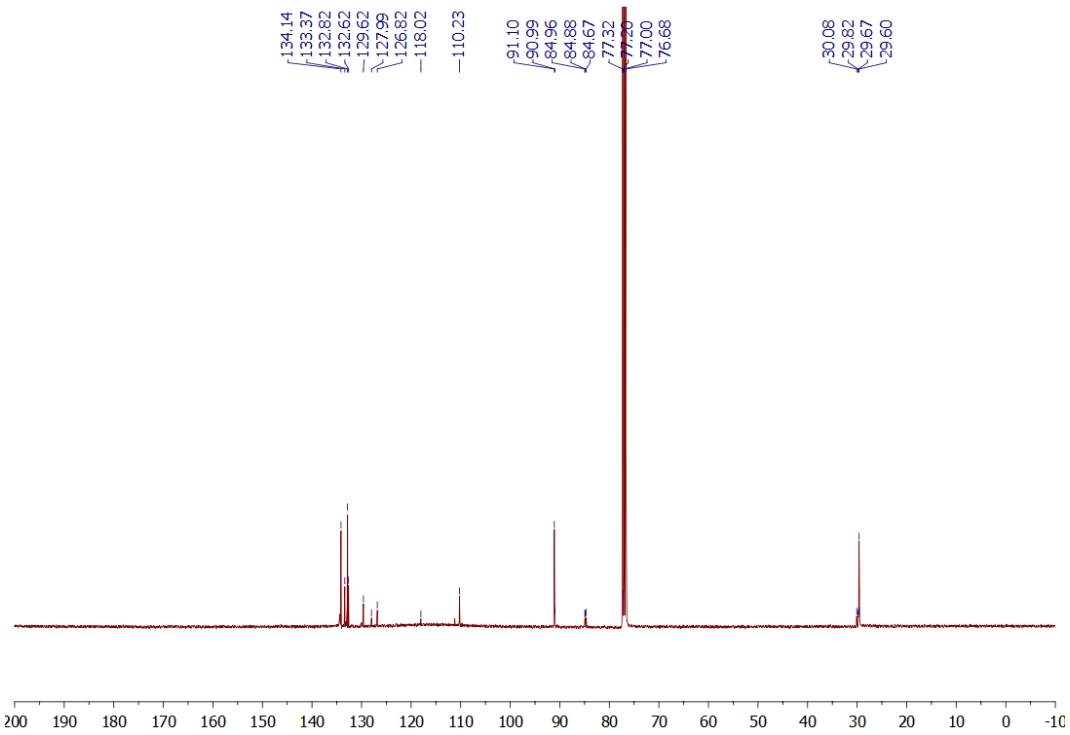

Figure S14 Complex **9**: ^{13}C NMR spectrum

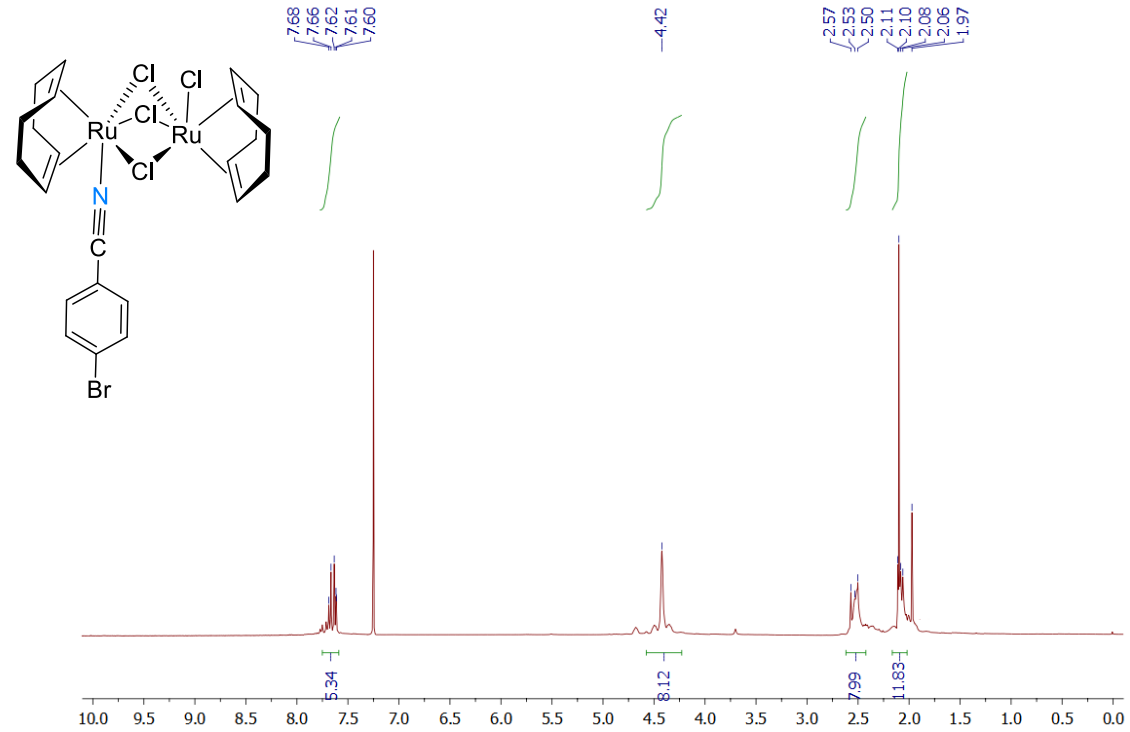

Figure S15 Complex **9b**: ^{1}H NMR spectrum

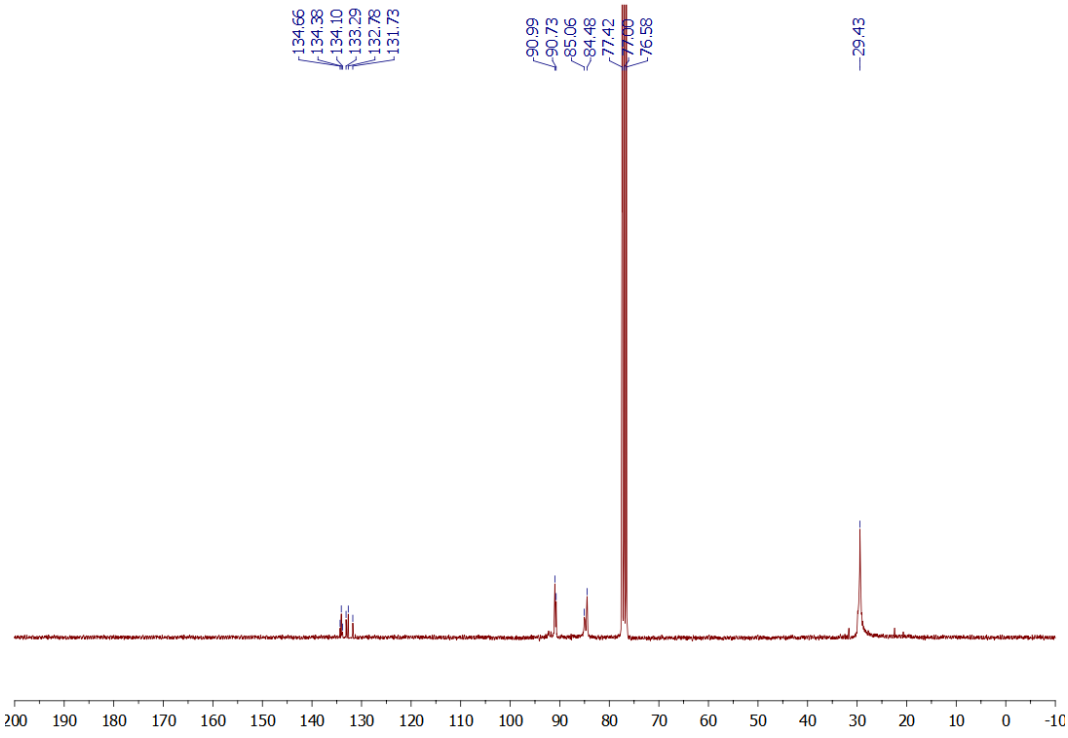

Figure S16 Complex **9b**: ^{13}C NMR spectrum

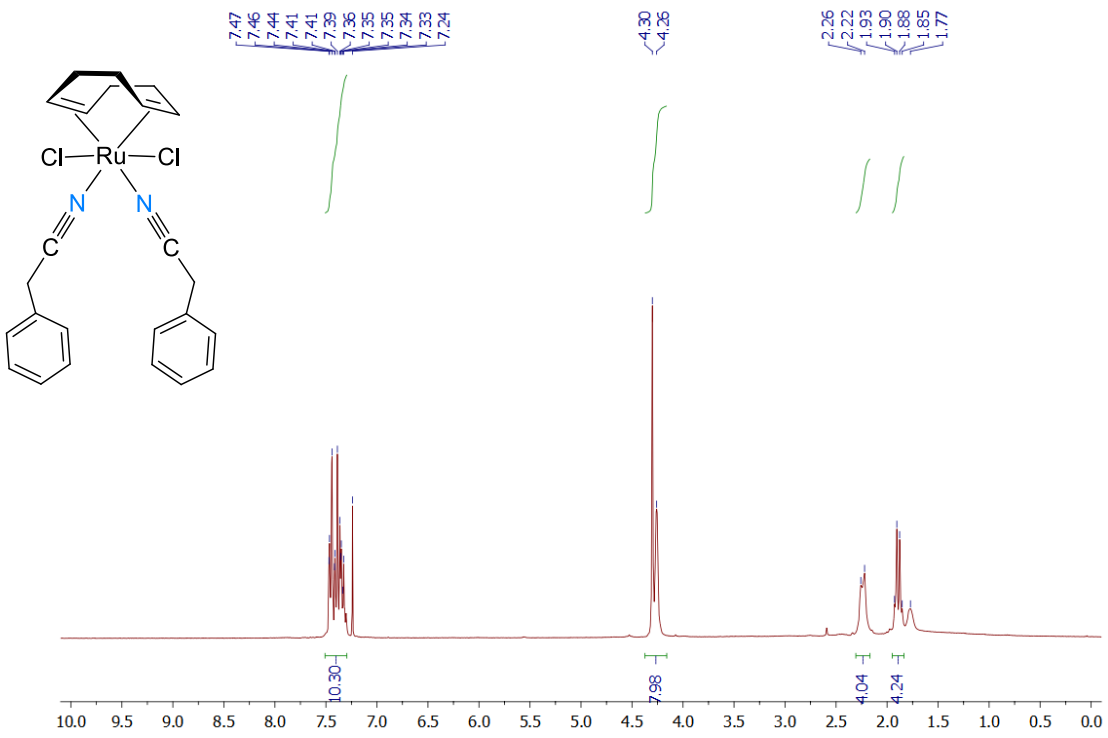

Figure S17 Complex **10**: ^{1}H NMR spectrum

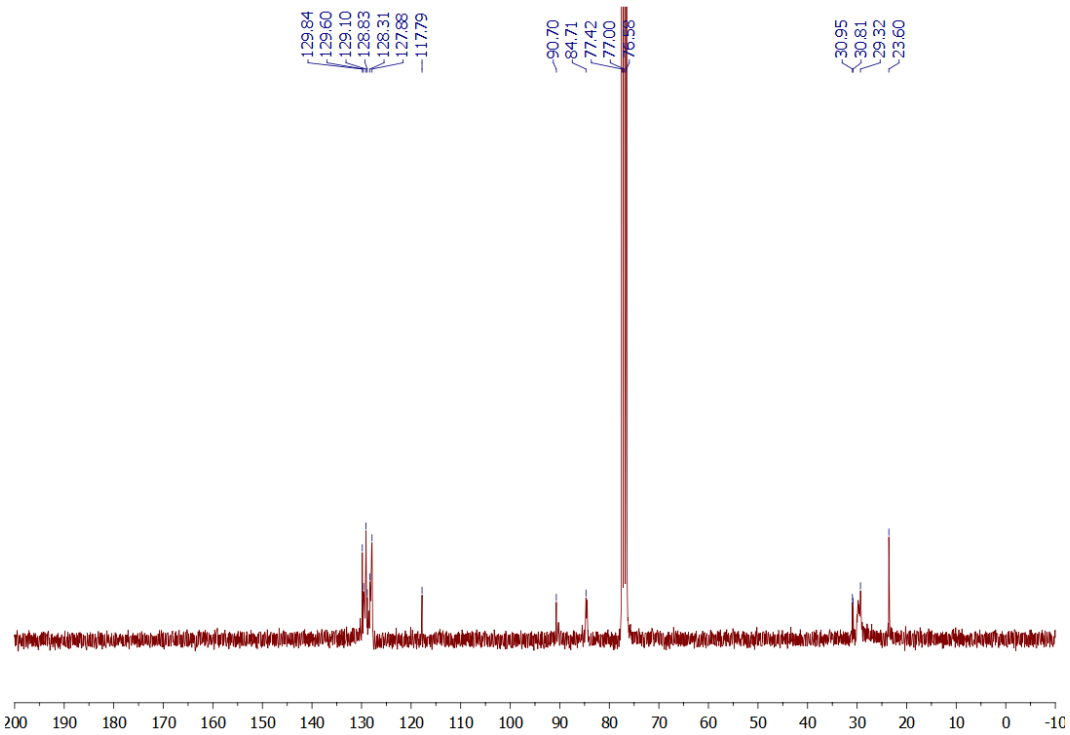

Figure S18 Complex **10**: ^{13}C NMR spectrum

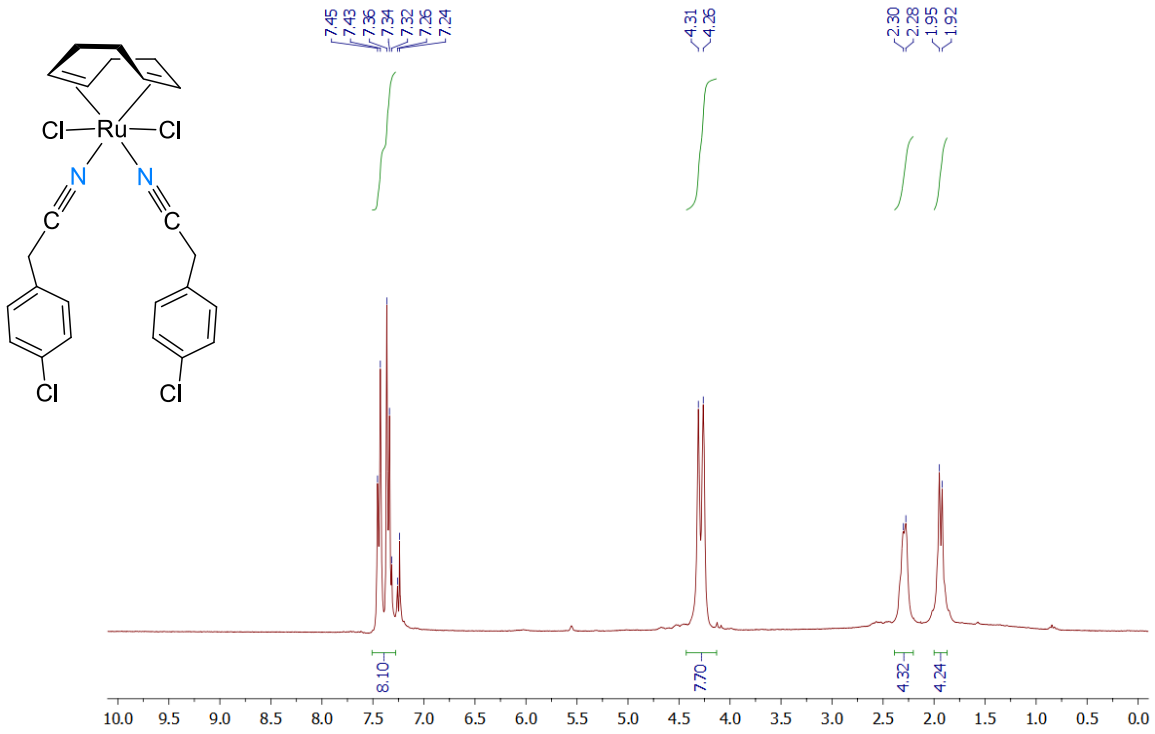

Figure S19 Complex **11**: ^{1}H NMR spectrum

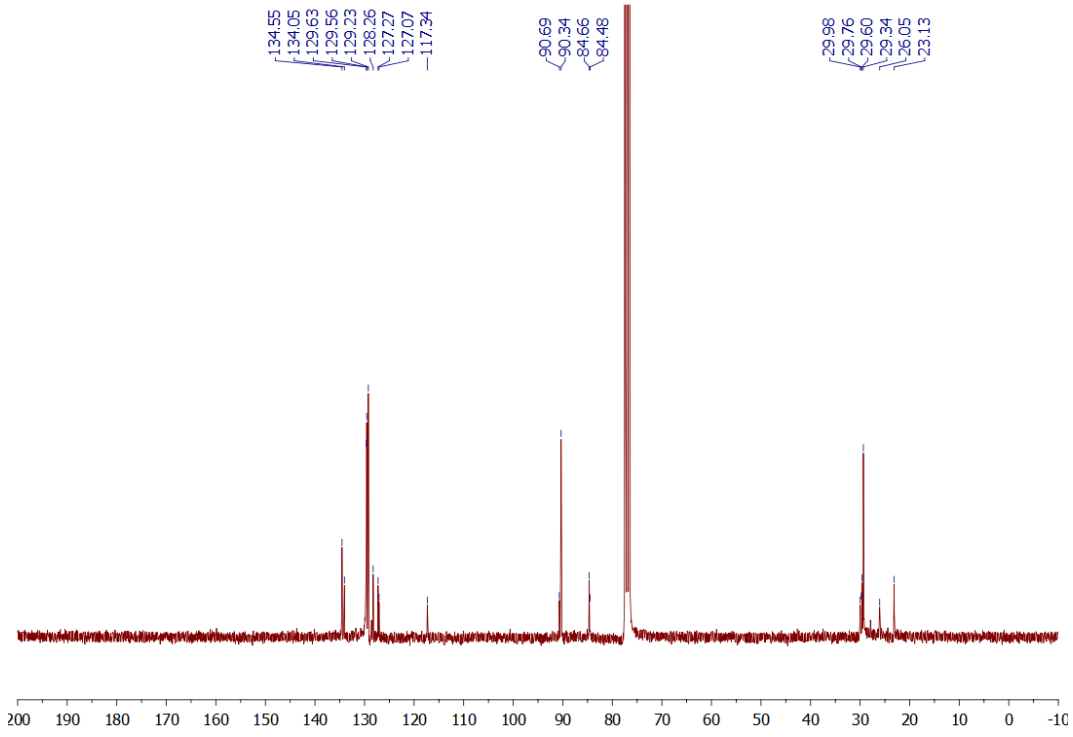

Figure S20 Complex **11**: ^{13}C NMR spectrum

3. Crystallographic data and structure refinement parameters (Tables S1-S5).

Table S1. Crystal data and structure refinement for **1**, **2**, **3**, and **4**.

Complex	1	2	3	4
Emp. formula	$C_{14}H_{22}N_2Cl_6Ru$	$C_{15}H_{23}N_2Cl_5Ru$	$C_{16}H_{22}N_2Cl_2Ru$	$C_{17}H_{27.8}N_2O_{0.4}Cl_5Ru$
CCDC Identifier	2150078	2150088	2150089	2150080
Form. weight (g.mol^{-1})	532.1	509.67	414.32	544.93
Crystal system	monoclinic	monoclinic	monoclinic	triclinic
Space group	$P2_1/m$	$P2_1/c$	$P2_1/n$	P-1
Crystal descr.	yellow block	yellow rod	yellow block	yellow block
a (Å)	10.7406(4)	13.88650(10)	10.30500(10)	8.4685(2)
b (Å)	9.7195(2)	12.67670(10)	11.55420(10)	9.06700(10)
c (Å)	11.0048(4)	11.78890(10)	14.9460(2)	15.2944(2)
α (°)	90	90	90	103.8080(10)
β (°)	116.627(4)	102.7890(10)	103.3470(10)	97.124(2)
γ (°)	90	90	90	96.5140(10)
Volume (Å^3)	1026.99(3)	2023.78(3)	1731.49(3)	1119.08(3)
Z	4	4	4	2
Abs. coeff. (m.mm^{-1})	1.543	12.335	10.114	11.208
F(000)	532.0	1024.0	840.0	552.0
Independent refl.	2939	4167	3652	4411
Completeness (%)	100	100	100	100
Data/Restr/Para	2939/0/133	4167/0/210	3652/0/190	4411/0/242
Goodness of fit on F^2	1.061	1.045	1.092	1.046
Final R_1 indexes	0.0318	0.0399	0.0453	0.0623
wR_2 indices (all data)	0.0762	0.1056	0.1252	0.1660
Largest diffr. peak and hole (e.Å^{-3})	1.28/-1.00	1.02/-2.28	1.44/-1.25	2.10/-1.45

Table S2. Crystal data and structure refinement for **5**, **6**, **7**, and **8**.

Complex	5	6	7	8
Emp. formula	$C_{30}H_{46}N_6Cl_4Ru_2$	$C_{14}H_{22}N_2O_2Cl_2Ru$	$C_{12}H_{16}N_2Cl_4Ru$	$C_{22}H_{22}N_2Cl_2Ru$
CCDC Identifier	2150082	2150084	2150087	2150079
Form. weight (g.mol^{-1})	418.36	420.29	431.14	486.38
Crystal system	triclinic	monoclinic	monoclinic	monoclinic
Space group	P-1	$P2_1/n$	$P2_1/n$	$C2/c$
Crystal descr.	yellow block	orange block	yellow rod	orange block
a (Å)	10.5410(2)	7.48061(19)	7.20380(10)	19.8130(3)
b (Å)	12.8885(2)	12.1203(3)	18.34300(10)	7.62670(10)
c (Å)	13.7574(2)	18.7072(5)	11.74880(10)	14.1347(2)
α (°)	87.9940(10)	90	90	90
β (°)	87.4260(10)	100.208(2)	101.8550(10)	102.0560(10)
γ (°)	75.9940(10)	90	90	90
Volume (Å^3)	1811.09(5)	1669.28(7)	1519.36(3)	2088.75(5)
Z	2	4	4	8
Abs. coeff. (m.mm^{-1})	9.670	1.264	14.715	8.487
F(000)	848.0	856.0	856.0	984.0
Independent refl.	7601	3543	3138	2156
Completeness (%)	100	100	100	100
Data/Restr/Para	7601/36/391	3543/0/192	3138/0/173	2156/0/123
Goodness of fit on F^2	1.048	1.030	1.099	1.067
Final R_1 indexes	0.0395	0.0310	0.0257	0.0365
wR_2 indices (all data)	0.1006	0.0825	0.0672	0.0987
Largest diffr. peak and hole (e.Å^{-3})	1.04/-1.12	0.89/-0.86	0.95/-0.96	1.77/-1.32

Table S3. Crystal data and structure refinement for **9**, **9b**, **10**, and **11**.

Complex	9	9b	10	11
Emp. formula	$C_{27}H_{32}N_2O_{0.26}Cl_2Br_2Ru$	$C_{50}H_{64}N_2O_2Cl_8Br_2Ru_4$	$C_{48}H_{52}N_4Cl_4Ru_2$	$C_{48}H_{52}N_4Cl_4Ru_2$
CCDC Identifier	2150081	2150083	2150086	2150085
Form. weight (g.mol^{-1})	748.36	1572.73	514.44	514.44
Crystal system	monoclinic	triclinic	orthorhombic	monoclinic
Space group	*C*2/c	*P*-1	*P*bca	$P2_1/c$
Crystal descr.	yellow block	yellow rod	orange block	yellow block
a (Å)	14.3588(4)	12.8817(2)	14.13770(10)	14.2530(2)
b (Å)	10.5613(3)	14.1362(2)	24.17560(10)	25.6766(3)
c (Å)	19.5258(5)	17.16770(10)	26.43830(10)	13.88990(10)
α (°)	90	87.3840(10)	90	90
β (°)	97.076(2)	76.4210(10)	90	106.0360(10)
γ (°)	90	64.5740(10)	90	90
Volume (Å^3)	2938.49(14)	2739.06(6)	9036.28(8)	4885.47(10)
Z	8	2	8	4
Abs. coeff. (m.mm^{-1})	3.459	14.385	7.879	9.330
F(000)	1488.0	1552.0	4192.0	2352.0
Independent refl.	3007	10777	9391	10339
Completeness (%)	100	100	100	100
Data/Restr/Para	3007/0/168	10777/0/615	9391/0/523	10339/0/559
Goodness of fit on F^2	1.113	1.048	1.084	1.047
Final R_1 indexes	0.0464	0.0413	0.0315	0.0443
wR_2 indices (all data)	0.1092	0.1131	0.0857	0.1199
Largest diffr. peak and hole (e.Å^{-3})	1.95/-1.43	2.00/-1.31	0.82/-1.40	1.87/-0.86

Table S4. Selected bond lengths and angles for **1-6**.

Description	1[a]	2	3	4	5	6
Ru1-C1	2.214(2)	2.208(3)	2.223(4)	2.218(5)	2.222(4)	2.221(3)
Ru1-C2	2.216(2)	2.215(3)	2.215(4)	2.220(5)	2.215(4)	2.214(3)
Ru1-C5	2.216(2)	2.219(3)	2.213(4)	2.219(5)	2.212(3)	2.222(3)
Ru1-C6	2.214(2)	2.228(3)	2.215(4)	2.219(5)	2.206(3)	2.221(3)
Ru1-Cl1	2.4276(5)	2.4179(7)	2.4256(10)	2.4207(13)	2.4065(10)	2.4187(7)
Ru1-Cl2	2.4276(5)	2.4271(7)	2.4245(10)	2.4072(11)	2.4222(9)	2.4123(7)
Ru1-N1	2.051(3)	2.025(3)	2.039(3)	2.036(4)	2.043(3)	2.029(2)
Ru1-N2	2.029(3)	2.038(2)	2.029(4)	2.033(4)	2.039(3)	2.032(2)
C1-C2	1.383(3)	1.379(5)	1.378(6)	1.374(8)	1.384(5)	1.382(4)
C2-C3	1.513(3)	1.519(6)	1.498(6)	1.536(10)	1.523(6)	1.511(4)
C3-C4	1.518(5)	1.503(7)	1.488(7)	1.488(10)	1.538(6)	1.537(5)
N1-C$_x$[b]	1.133(3)	1.130(5)	1.129(5)	1.130(6)	1.133(5)	1.137(4)
Ru1-C1-C8	112.01(16)	112.2(2)	112.6(3)	110.8(3)	110.7(2)	112.6(2)
C1-Ru1-C6	90.74(7)	79.73(13)	79.79(17)	80.2(2)	80.50(14)	79.87(12)
N1-Ru1-N2	163.92(11)	164.03(11)	165.11(14)	165.74(16)	165.42(13)	165.65(9)
N1-Ru1-Cl1	84.38(5)	84.30(8)	84.33(10)	85.06(11)	86.68(9)	85.69(7)
N1-Ru1-C1	78.63(9)	77.49(13)	78.61(16)	77.37(17)	77.64(13)	77.26(10)
N2-Ru1-C2	76.95(9)	78.30(12)	76.58(15)	78.37(18)	77.41(14)	78.43(10)
Cl1-Ru1-Cl2	93.64(3)	92.73(3)	95.08(4)	93.05(4)	94.08(4)	92.60(3)
C1-C2-C3	123.5(2)	121.8(4)	123.6(4)	122.7(6)	122.2(4)	123.2(3)
N1-C$_x$-C$_{xx}$[b,c]	179.1(4)	174.9(4)	178.1(5)	176.9(5)	177.0(4)	175.6(3)
N2-C$_x$-C$_{xx}$[b,c]	178.3(4)	179.0(3)	173.2(5)	175.9(5)	177.3(5)	178.1(3)
Ru1-N1-C$_x$[b]	170.7(3)	173.8(1)	175.3(4)	174.4(4)	176.4(3)	175.7(2)
Ru1-N2-C$_x$[b]	176.8(3)	174.4(2)	177.5(4)	174.1(4)	176.2(3)	173.6(2)
Ru1-N1-C$_x$-C$_{xx}$[b,c]	0.0(9)	-81.4(6)	165.6(6)	120.5(6)	49.8(8)	-40.4(4)
N1-Ru1-N2-C$_x$[b]	0.0(5)	-4.7 (5)	66.4(5)	65.5(5)	8.9(6)	42.1(5)
Cl1-Ru1-C1-C8	-47.0 (8)	48.7 (6)	152.2(7)	-144.6(7)	145.3(4)	-157.5(5)
C1-C2-C3-C4	-70.7 (6)	83.3(5)	63.5(6)	-86.1(7)	91.1(4)	-53.7(4)
C8-C1-C2-C3	0.3(9)	0.9(5)	0.4(6)	1.2(8)	-3.1(5)	-1.5(4)

[a] Half a molecule is present in the unit cell. Therefore, some labels such as N2 and Cl2 refers to the symmetry related N1 and Cl1 (depending on the type of symmetry present). [b] C_x = carbon atom adjacent to nitrogen carbon of the nitrile ligand. [c] C_{xx} = carbon atom adjacent to C_x of the nitrile ligand.

Table S5. Selected bond lengths and angles for **7**-**11**, and **9b**.

Description	7	8[a]	9[a]	9b	10	11
Ru1-C1	2.215(2)	2.215(3)	2.212(4)	2.201(3)	2.215(2)	2.225(4)
Ru1-C2	2.228(2)	2.222(3)	2.213(4)	2.203(3)	2.212(2)	2.212(4)
Ru1-C5	2.221(2)	2.222(3)	2.212(4)	2.222(3)	2.206(2)	2.206(4)
Ru1-C6	2.231(2)	2.215(3)	2.213(4)	2.206(3)	2.216(2)	2.211(4)
Ru1-Cl1	2.4128(6)	2.4264(7)	2.4232(11)	2.3830(8)	2.4272(5)	2.4347(10)
Ru1-Cl2	2.4344(6)	2.4264(7)	2.4232(11)	2.4347(8)[d]	2.4132(5)	2.4156(10)
Ru1-N1	2.024(2)	2.021(3)	2.022(4)	2.021(3)	2.0366(19)	2.032(3)
Ru1-N2	2.041(2)	2.021(3)	2.022(4)	-	2.0344(19)	2.044(4)
C1-C2	1.388(4)	1.381(4)	1.376(7)	1.390(5)	1.378(3)	1.372(6)
C2-C3	1.522(3)	1.508(5)	1.511(6)	1.514(5)	1.530(3)	1.512(6)
C3-C4	1.542(4)	1.510(6)	1.544(7)	1.532(6)	1.540(3)	1.548(6)
N1-C$_x$[b]	1.135(3)	1.133(4)	1.142(6)	1.139(5)	1.136(3)	1.137(5)
Ru1-C1-C8	111.41(16)	111.9(2)	112.9(3)	112.8(2)	110.89(15)	113.2(3)
C1-Ru1-C6	79.84(9)	80.54(12)	80.20(17)	80.49(14)	80.24(9)	79.31(16)
N1-Ru1-N2	166.85(8)	162.66(15)	166.1(2)	-	164.68(7)	163.84(14)
N1-Ru1-Cl1	85.71(6)	83.77(7)	86.10(10)	86.16(9)[d]	86.00(5)	84.57(10)
N1-Ru1-C1	77.78(9)	78.79(11)	76.87(17)	78.77(13)[d]	78.17(8)	113.26(15)
N2-Ru1-C2	76.61(9)	77.81(11)	76.87(17)	-	77.24(8)	113.56(15)
Cl1-Ru1-Cl2	94.33(2)	95.61(4)	92.45(6)	84.66(3)[e]	93.226(19)	91.25(4)
C1-C2-C3	123.1(2)	123.8(3)	123.5(5)	124.7(3)	122.9(2)	122.6(4)
N1-C$_x$-C$_{xx}$[b,c]	174.9(3)	177.3(3)	175.1(5)	177.2(4)	175.5(3)	179.5(5)
N2-C$_x$-C$_{xx}$[b,c]	176.2(3)	177.3(3)	175.1(5)	-	175.6(2)	178.1(5)
Ru1-N1-C$_x$[b]	176.2(2)	170.3(3)	178.2(4)	171.5(3)	172.43(19)	177.5(3)
Ru1-N2-C$_x$[b]	177.0(2)	170.3(3)	178.2(4)	-	178.21(18)	168.6(3)
Ru1-N1-C$_x$-C$_{xx}$[b,c]	53.5(4)	29.6(5)	132.0(4)	17.4(6)	30.2(4)	20.1(5)
N1-Ru1-N2-C$_x$[b]	-28.9(3)	-6.5(4)	17.3(5)	-	2.0(5)	14.0(7)
Cl1-Ru1-C1-C8	143.4(4)	150.7(4)	155.9(5)	-153.4(5)[f]	145.4(3)	-158.4(5)
C1-C2-C3-C4	89.2(4)	-71.1(4)	-90.4(4)	-48.7(5)	88.4(3)	-52.4(5)
C8-C1-C2-C3	-0.8(5)	0.9(5)	2.2(5)	-2.3(5)	-2.6(4)	-1.9(6)

[a] Half a molecule is present in the unit cell. Therefore, some labels such as N2 and Cl2 refers to the symmetry related N1 and Cl1 (depending on the type of symmetry present). [b] C_x = carbon atom adjacent to nitrogen carbon of the nitrile ligand. [c] C_{xx} = carbon atom adjacent to C_x of the nitrile ligand. [d] Bridging chloride ligand. [e] Cl1 (terminal chloride), Cl2 (bridging chloride). [f] Cl2-Ru1-C1-C8.

4. Molecular overlay and packing diagrams (Figures S21-S22).

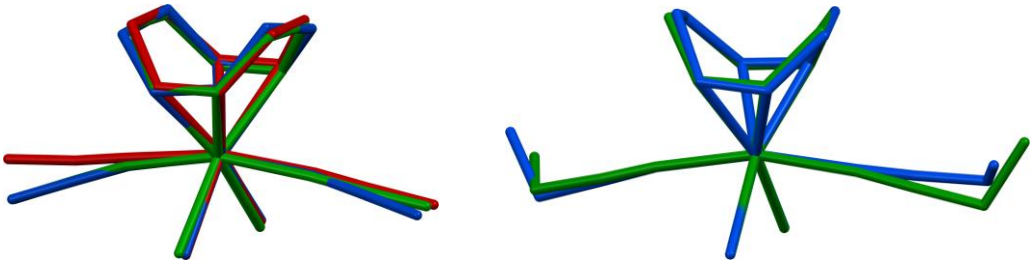

Figure S21. Molecular overlay diagrams of the structures of **1** (left: green (this work), red (CCDC refcode GAYBAJ), blue (CCDC refcode AWOQEJ)), and **2** (right: green (this work), blue (AZINON)). Mean RMS in **1**: 0.024 (red and blue), 0.00815 (red and green), 0.0168 (green and blue). Mean RMS in **2**: 0.00499.

Table S6. Packing diagrams of complexes **1**, **1** (Singleton, Chirririwa), **2**, and **2** (Chirririwa).

Description	**View along crystallographic axis**		
	a	*b*	*c*
1	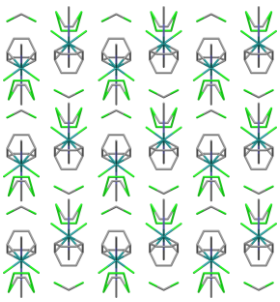	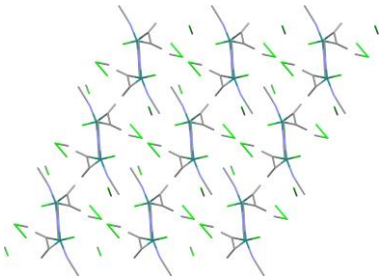	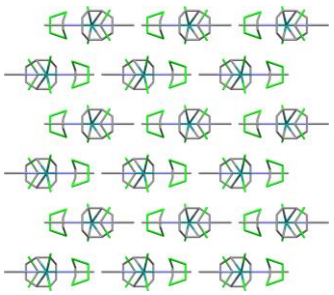
1 (Singleton)	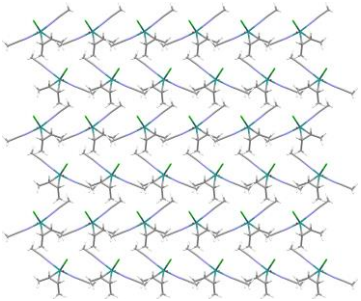	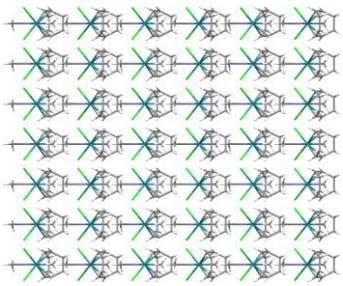	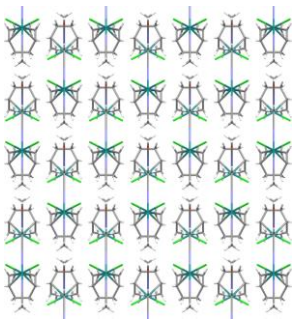
1 (Chirririwa)	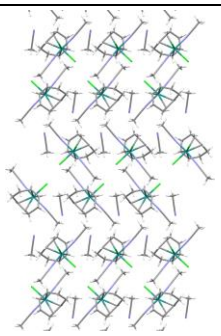	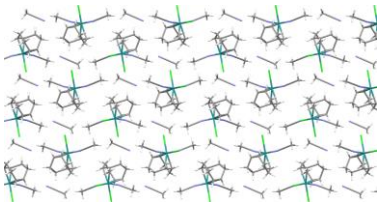	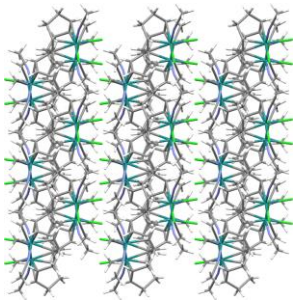
2	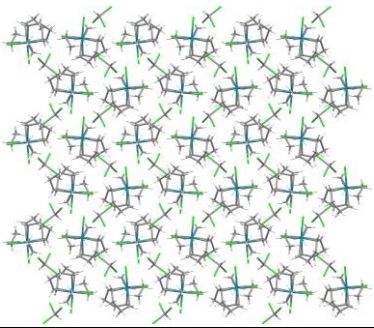	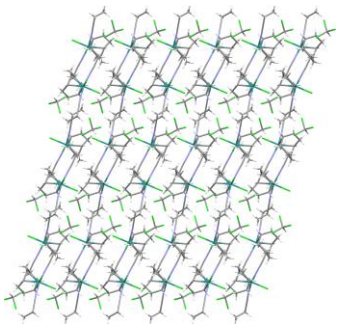	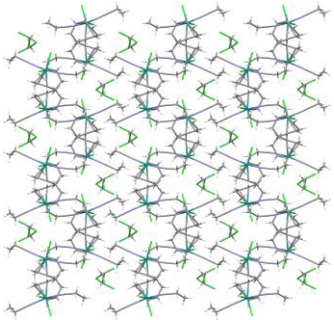
2 (Chirririwa)	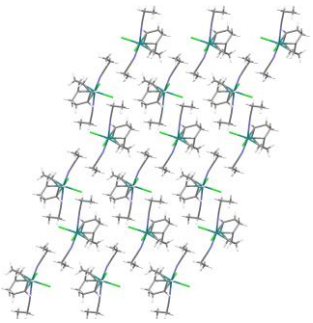	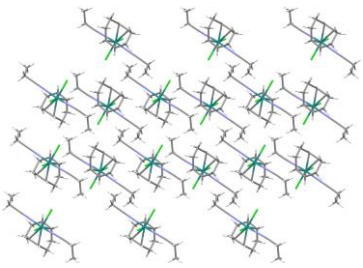	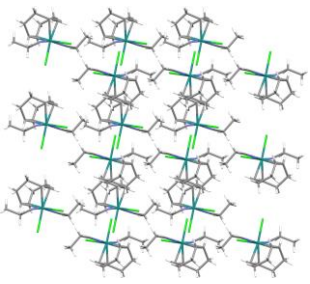

5. Electrochemistry (Figure S22, Table S7).

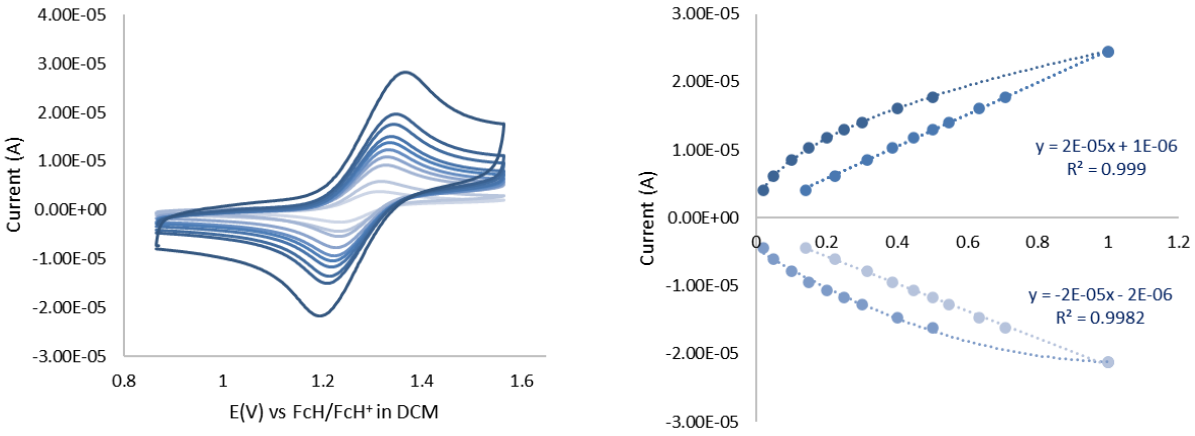

Figure S22. (Left) Cyclic voltammograms of complex **2** at scan rates of 0.02 (light blue, lowest peak current), 0.10, 0.15, 0.20, 0.25, 0.30, 0.4, 0.50, and 1.00 (dark blue, highest peak current) $V.s^{-1}$. Scans were initiated in the positive direction. **Figure S23.** (Right) The linear relationship between peak currents (i_p) and $(\text{scan rate})^{½}$ for the oxidation (dark blue) and reduction (light blue) of complex **2**, as described by the Randles-Sevcik equation. The dependence of i_{pa} and i_{pc} on scan rate ($V.s^{-1}$).

Table S7. Electrochemical data (*vs.* FcH/FcH^+) of complex **2** in DCM at indicated scan rates.

Scan rate ($V.^{s-1}$)	Epa (V)	Epc (V)	ΔE (V)	E^o (V)	i_{pa} (A)	i_{pc} (A)	i_{pc}/i_{pa}
0.02	1.319	1.240	0.079	1.280	4.07E-06	-4.44E-06	1.09
0.05	1.320	1.239	0.081	1.280	6.11E-06	-6.11E-06	1.00
0.1	1.332	1.238	0.094	1.285	8.52E-06	-7.78E-06	0.91
0.15	1.333	1.237	0.096	1.285	1.04E-05	-9.44E-06	0.91
0.2	1.335	1.234	0.101	1.285	1.19E-05	-1.07E-05	0.91
0.25	1.340	1.227	0.113	1.284	1.30E-05	-1.17E-05	0.90
0.3	1.347	1.213	0.134	1.280	1.41E-05	-1.28E-05	0.91
0.4	1.349	1.208	0.141	1.279	1.61E-05	-1.46E-05	0.91
0.5	1.351	1.201	0.150	1.276	1.78E-05	-1.61E-05	0.91
1	1.398	1.194	0.204	1.296	2.44E-05	-2.13E-05	0.87

6. Catalysis (Figure S23).

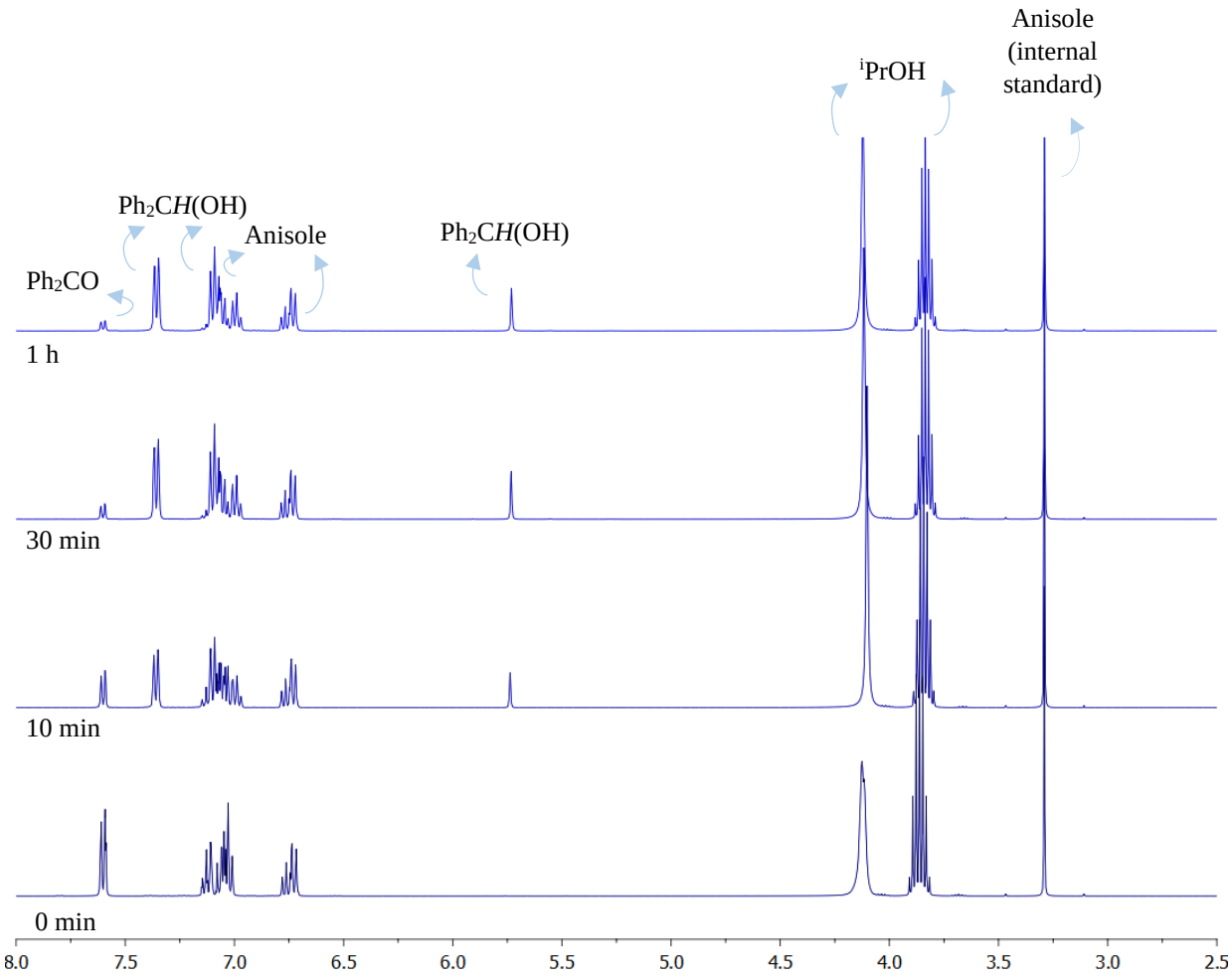

Figure S21 ^{1}H NMR spectrum of catalysis reaction mixture obtained in C_6D_6 at the indicated time intervals. General reaction conditions: Ph_2CO (18 mg, 0.1 mmol), ^{i}PrOH (100 µL), KO^{t}Bu (10 mol%), Ru catalyst (3 mol%), anisole (11 µl, 0.1 mmol), C_6D_6, 80 °C, 30 min.

7. References

[1] T. V. Ashworth, D. C. Liles, D. J. Robinson, E. Singleton, N. J. Coville, E. Darling, A. J. Markwell, *S. Afr. J. Chem.* **1987**, *40*, 183-188.

[2] A. Ali, F. P. Malan, E. Singleton, R. Meijboom, *Organometallics* **2014**, *33*, 5983-5989.

[3] O. Rigaku, CrysAlis PRO Software system. Rigaku Corporation. Oxford, UK: 2018.

[4] G. M. Sheldrick, *Acta Crystallogr. A* **2015**, *71* (1), 3-8.

[5] G. M. Sheldrick, *Acta Crystallogr. C* **2015**, *71* (1), 3-8.

[6] E. Magdzinski, P. Gobbo, C. D. Martin, M. S. Workentin, P. J. Ragogna, *Inorg. Chem.* **2012**, *51*, 8425-8432.

[7] M. J. Frisch, G. W. Trucks, H. B. Schlegel, G. E. Scuseria, M. A. Robb, J. R. Cheeseman, G. Scalmani, V. Barone, G. A. Petersson, H. Nakatsuji, X. Li, M. Caricato, A. V. Marenich, J. Bloino, B. G. Janesko, R. Gomperts, B. Mennucci, H. P. Hratchian, J. V. Ortiz, A. F. Izmaylov, J. L. Sonnenberg, D. Williams-Young, F. Ding, F. Lipparini, F. Egidi, J. Goings, B. Peng, A. Petrone, T. Henderson, D. Ranasinghe, V. G. Zakrzewski, J. Gao, N. Rega, G. Zheng, W. Liang, M. Hada, M. Ehara, K. Toyota, R. Fukuda, J. Hasegawa, M. Ishida, T. Nakajima, Y. Honda, O. Kitao, H. Nakai, T. Vreven, K. Throssell, J. A. Montgomery, Jr., J. E. Peralta, F. Ogliaro, M. J. Bearpark, J. J. Heyd, E. N. Brothers, K. N. Kudin, V. N. Staroverov, T. A. Keith, R. Kobayashi, J. Normand, K. Raghavachari, A. P. Rendell, J. C. Burant, S. S. Iyengar, J. Tomasi, M. Cossi, J. M. Millam, M. Klene, C. Adamo, R. Cammi, J. W. Ochterski, R. L. Martin, K. Morokuma, O. Farkas, J. B. Foresman, and D. J. Fox, Gaussian, Inc., Wallingford CT, 2016.

[8] F. Weigend, R. Ahlrichs, *Phys. Chem. Chem. Phys.* **2005**, *7*, 3297-3305.

[9] Grimme, S., Semiempirical GGA-type density functional constructed with a long-range dispersion correction. *J. Comput. Chem.* **2006**, *27*, 1787-1799.

[10] Chemcraft – graphical software for visualization of quantum chemistry computations. https://www.chemcraftprog.com.